

Stoichiometry dependent Co³⁺ Spin State in La_xSr_{2-x}CoGaO_{5+δ} brownmillerite phases.

Kun Luo and Michael A. Hayward

Supporting Information

Sample	Space group	χ^2	wRp (%)	Rp (%)
La _{0.5} Sr _{1.5} CoGaO _{5.01}	I2mb	2.261	1.41	2.25
	<i>Imma</i>	17.31	3.91	4.73
La _{0.6} Sr _{1.4} CoGaO _{5.02}	I2mb	2.917	1.46	2.18
	<i>Imma</i>	22.96	4.12	4.75
La _{0.7} Sr _{1.3} CoGaO _{5.05}	I2mb	3.474	2.64	2.22
	<i>Imma</i>	11.12	4.74	3.67
La _{0.8} Sr _{1.2} CoGaO _{5.09}	<i>I2mb</i>	4.986	2.19	2.97
	<i>Imma</i>	3.294	1.78	2.48

Table S1. Fitting statistics for the refinement of the brownmillerite models against neutron powder diffraction data collected from La_xSr_{2-x}CoGaO_{5+δ} (x = 0.5, 0.6, 0.7, 0.8) at room temperature.

Atom	site	x	y	z	fraction	U_{equiv} (\AA^2)
La/Sr(1)	8c	0.4953(1)	0.1084(1)	0.0167(1)	0.25/0.75	0.0070
Co/Ga(1)	4a	0.9999(4)	0	0	0.869(2)/ 0.131(2)	0.0122
Co/Ga(2)	4b	0.9576(4)	$\frac{1}{4}$	0.9299(1)	0.131(2)/ 0.869(2)	0.0048
O(1)	8c	0.2462(2)	0.9930(1)	0.2523(1)	1	0.0100
O(2)	8c	0.0185(4)	0.1462(1)	0.0531(1)	1	0.0148
O(3)	4b	0.6139(1)	$\frac{1}{4}$	0.8698(1)	1	0.0084

$\text{La}_{0.5}\text{Sr}_{1.5}\text{CoGaO}_5$ -space group $I2mb$.

$a = 5.4306(2)$ \AA , $b = 15.9579(7)$ \AA , $c = 5.6336(2)$ \AA , $V = 488.22(6)$ \AA^3

$\chi^2 = 2.261$, $wR_p = 1.41\%$, $R_p = 2.25\%$

Table S2a. The structure of $\text{La}_{0.5}\text{Sr}_{1.5}\text{CoGaO}_{5.01}$ refined against neutron powder diffraction data collected at room temperature.

Atom	U_{11}	U_{22}	U_{33}	U_{12}	U_{13}	U_{23}
La/Sr(1)	0.0064(1)	0.0064(1)	0.0081(1)	0.0001(1)	0.0004(2)	-0.0013(2)
Co/Ga(1)	0.0016(4)	0.0297(7)	0.0053(5)	0.0006(3)	0	0
Co/Ga(2)	0.0081(2)	0.0035(2)	0.0028(3)	0	-0.0004(2)	0
O(1)	0.0101(2)	0.0111(2)	0.0086(2)	-0.0012(3)	0.0011(1)	-0.0014(2)
O(2)	0.0141(3)	0.0096(2)	0.0206(3)	0.0068(2)	0.0034(2)	0.0067(2)
O(3)	0.0098(4)	0.0069(3)	0.0083(4)	0	-0.0004(2)	0

Table S2b. Anisotropic thermal parameters refined against neutron powder diffraction data collected from $\text{La}_{0.5}\text{Sr}_{1.5}\text{CoGaO}_{5.01}$ at room temperature

Atom	site	x	y	z	fraction	U_{equiv} (\AA^2)
La/Sr(1)	8c	0.4946(4)	0.1082(1)	0.0170(1)	0.3/0.7	0.0067
Co/Ga(1)	4a	0.9999(4)	0	0	0.872(2)/ 0.128 (2)	0.0112
Co/Ga(2)	4b	0.9575(1)	$\frac{1}{4}$	0.9302(1)	0.128(2)/ 0.872(2)	0.0053
O(1)	8c	0.2455(2)	0.9927(1)	0.2519(2)	1	0.0099
O(2)	8c	0.0187(1)	0.1462(1)	0.0542(1)	1	0.0151
O(3)	4b	0.6127(1)	$\frac{1}{4}$	0.8706(1)	1	0.0090
$\text{La}_{0.6}\text{Sr}_{1.4}\text{CoGaO}_5$ -space group $I2mb$. $a = 5.4326(2)$ \AA , $b = 15.9667(7)$ \AA , $c = 5.6402(2)$ \AA , $V = 489.22(3)$ \AA^3 $\chi^2 = 2.917$, $wRp = 1.46\%$, $Rp = 2.18\%$						

Table S3a. The structure of $\text{La}_{0.6}\text{Sr}_{1.4}\text{CoGaO}_{5.02}$ refined against neutron powder diffraction data collected at room temperature.

Atom	U_{11}	U_{22}	U_{33}	U_{12}	U_{13}	U_{23}
La/Sr(1)	0.0065(1)	0.0059(1)	0.0077(1)	0.0001(1)	0.0009(2)	-0.0010(2)
Co/Ga(1)	0.0011(5)	0.0276(8)	0.0046(5)	0.0001(1)	0	0
Co/ Ga(2)	0.0081(3)	0.0038(2)	0.0038(3)	0	-0.0001(1)	0
O(1)	0.0094(2)	0.0119(2)	0.0083(2)	-0.0009(3)	0.0009(2)	-0.0015(3)
O(2)	0.0142(3)	0.0105(2)	0.0205(4)	0.0072(2)	0.0035(3)	0.0066(3)
O(3)	0.0098(4)	0.0064(3)	0.0106(4)	0	-0.0043(3)	0

Table S3b. Anisotropic thermal parameters refined against neutron powder diffraction data collected from $\text{La}_{0.6}\text{Sr}_{1.4}\text{CoGaO}_{5.02}$ at room temperature.

Atom	site	x	y	z	fraction	U_{equiv} (\AA^2)
La/Sr(1)	8c	0.4942(1)	0.1079(1)	0.0169(1)	0.35/0.65	0.0063
Co/Ga(1)	4a	0.9999(7)	0	0	0.844(3)/ 0.156 (3)	0.0105
Co/Ga(2)	4b	0.9592(3)	$\frac{1}{4}$	0.9311(2)	0.156(3)/ 0.844(3)	0.0073
O(1)	8c	0.2475(3)	0.9924(1)	0.2523(3)	1	0.0084
O(2)	8c	0.0194(3)	0.1455(1)	0.0545(1)	1	0.0153
O(3)	4b	0.6108(3)	$\frac{1}{4}$	0.8719(2)	1	0.0105

$\text{La}_{0.7}\text{Sr}_{1.3}\text{CoGaO}_5$ -space group $I2mb$.

$a = 5.4445(9)$ \AA , $b = 15.9604(9)$ \AA , $c = 5.6411(8)$ \AA , $V = 490.19(30)$ \AA^3

$\chi^2 = 3.474$, $wR_p = 2.64$ %, $R_p = 2.22$ %

Table S4a. The structure of $\text{La}_{0.7}\text{Sr}_{1.3}\text{CoGaO}_{5.05}$ refined against neutron powder diffraction data collected at room temperature.

Atom	U_{11}	U_{22}	U_{33}	U_{12}	U_{13}	U_{23}
La/Sr(1)	0.0061(3)	0.0049(3)	0.0079(3)	0.0009(2)	0.0011(4)	0.0003(2)
Co/Ga(1)	0.0034(1)	0.0276(13)	0.0015(8)	-0.0001(1)	0	0
Co/Ga(2)	0.0087(6)	0.0050(5)	0.0082(8)	0	-0.0002(1)	0
O(1)	0.0070(4)	0.0118(5)	0.0059(3)	-0.0002(1)	0.0008(3)	0.0002(1)
O(2)	0.0158(5)	0.0133(5)	0.0168(7)	0.0075(4)	0.0023(5)	0.0065(6)
O(3)	0.0118(8)	0.0061(7)	0.0139(8)	0	-0.0046(6)	0

Table S4b. Anisotropic thermal parameters refined against neutron powder diffraction data collected from $\text{La}_{0.7}\text{Sr}_{1.3}\text{CoGaO}_{5.05}$ at room temperature.

Atom	site	x	y	z	fraction	U_{equiv} (\AA^2)
La/Sr(1)	8h	$\frac{1}{2}$	0.1081(1)	0.0169(1)	0.4/0.6	0.0074
Co/Ga(1)	4a	0	0	0	0.814(2)/ 0.186(2)	0.0136
Co/Ga(2)	8i	0.9596(1)	$\frac{1}{4}$	0.9315(1)	0.093(1)/ 0.407 (1)	0.0071
O(1)	8g	$\frac{1}{4}$	0.9923(1)	$\frac{1}{4}$	1	0.0095
O(2)	8h	0	0.1449(1)	0.0550(1)	1	0.0233
O(3)	8i	0.6151(1)	$\frac{1}{4}$	0.8716(2)	0.5	0.0131

$\text{La}_{0.8}\text{Sr}_{1.2}\text{CoGaO}_5$ -space group *Imma*.

$a = 5.4606(3)$ \AA , $b = 15.9329(11)$ \AA , $c = 5.6468(4)$ \AA , $V = 491.29(10)$ \AA^3

$\chi^2 = 3.294$, $wR_p = 1.78\%$, $R_p = 2.48\%$

Table S5a. The structure of $\text{La}_{0.8}\text{Sr}_{1.2}\text{CoGaO}_{5.09}$ refined against neutron powder diffraction data collected at room temperature.

Atom	U_{11}	U_{22}	U_{33}	U_{12}	U_{13}	U_{23}
La/Sr(1)	0.0082(2)	0.0058(1)	0.0080(1)	-0.0004(1)	0	0
Co/Ga(1)	0.0028(5)	0.0307(8)	0.0071(5)	0.0078(6)	0	0
Co/Ga(2)	0.0126(4)	0.0061(3)	0.0026(6)	0	0.0012(3)	0
O(1)	0.0077(2)	0.0143(3)	0.0064(2)	0	0.0001(1)	0
O(2)	0.0124(3)	0.0141(3)	0.0433(4)	0.0076(2)	0	0
O(3)	0.0146(5)	0.0049(5)	0.0198(6)	0	-0.0077(4)	0

Table S5b. Anisotropic thermal parameters refined against neutron powder diffraction data collected from $\text{La}_{0.8}\text{Sr}_{1.2}\text{CoGaO}_{5.09}$ at room temperature.

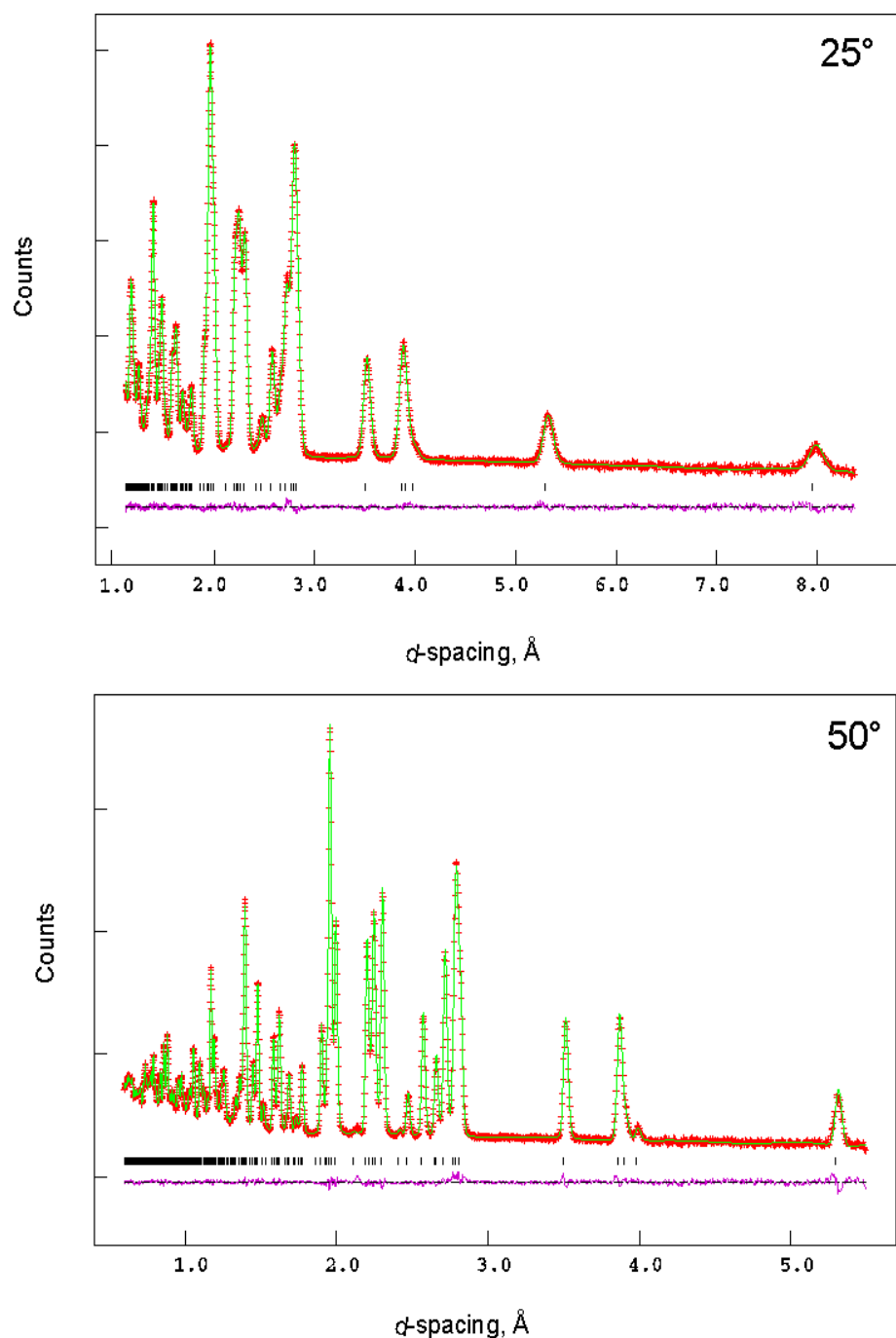


Figure S1a. Observed, calculated and difference plots from the refinement of $\text{La}_{0.5}\text{Sr}_{1.5}\text{CoGaO}_{5.01}$ against powder neutron diffraction data, 25° and 50° banks.

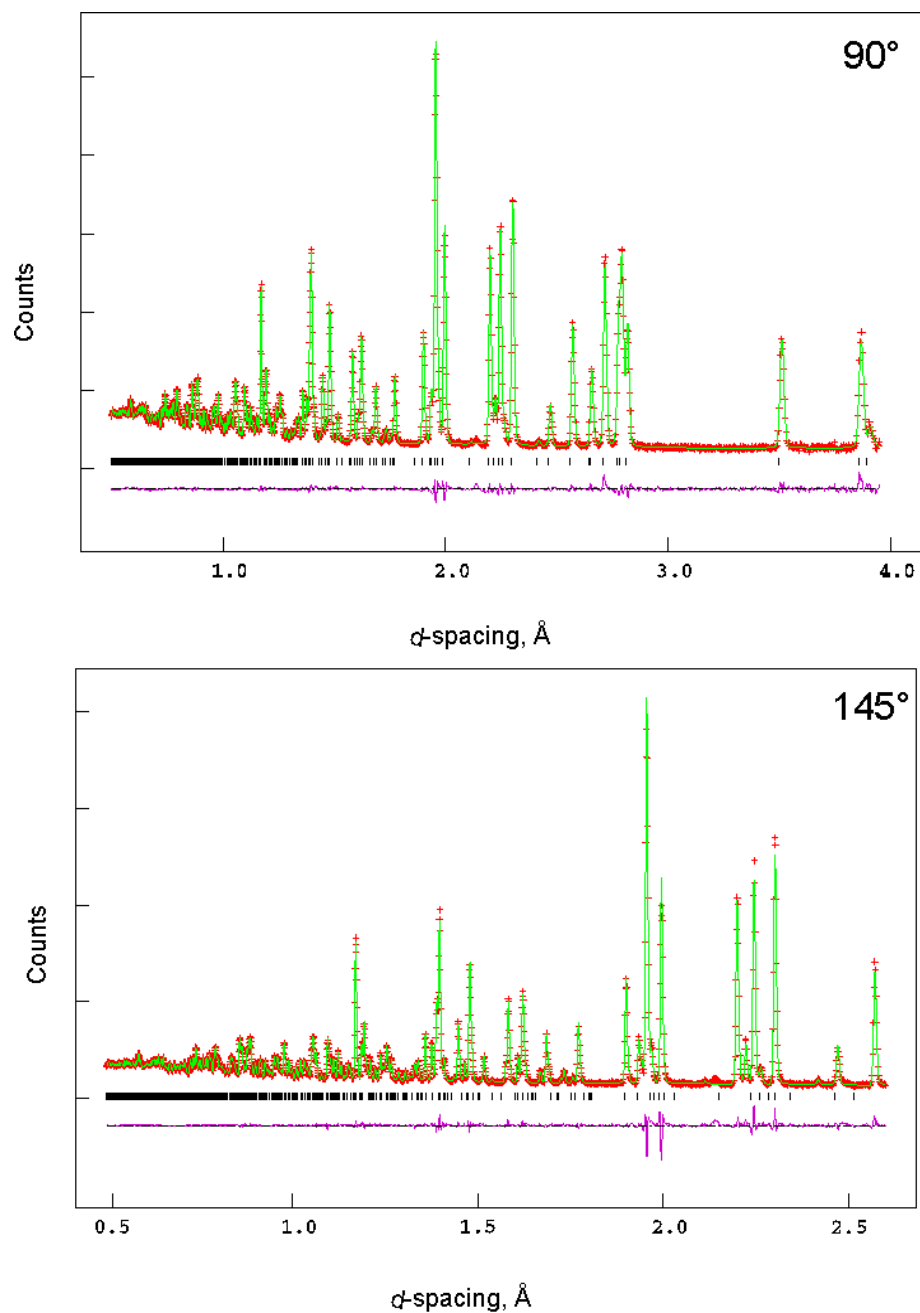


Figure S1b. Observed, calculated and difference plots from the refinement of $\text{La}_{0.5}\text{Sr}_{1.5}\text{CoGaO}_{5.01}$ against powder neutron diffraction data, 90° and 145° banks.

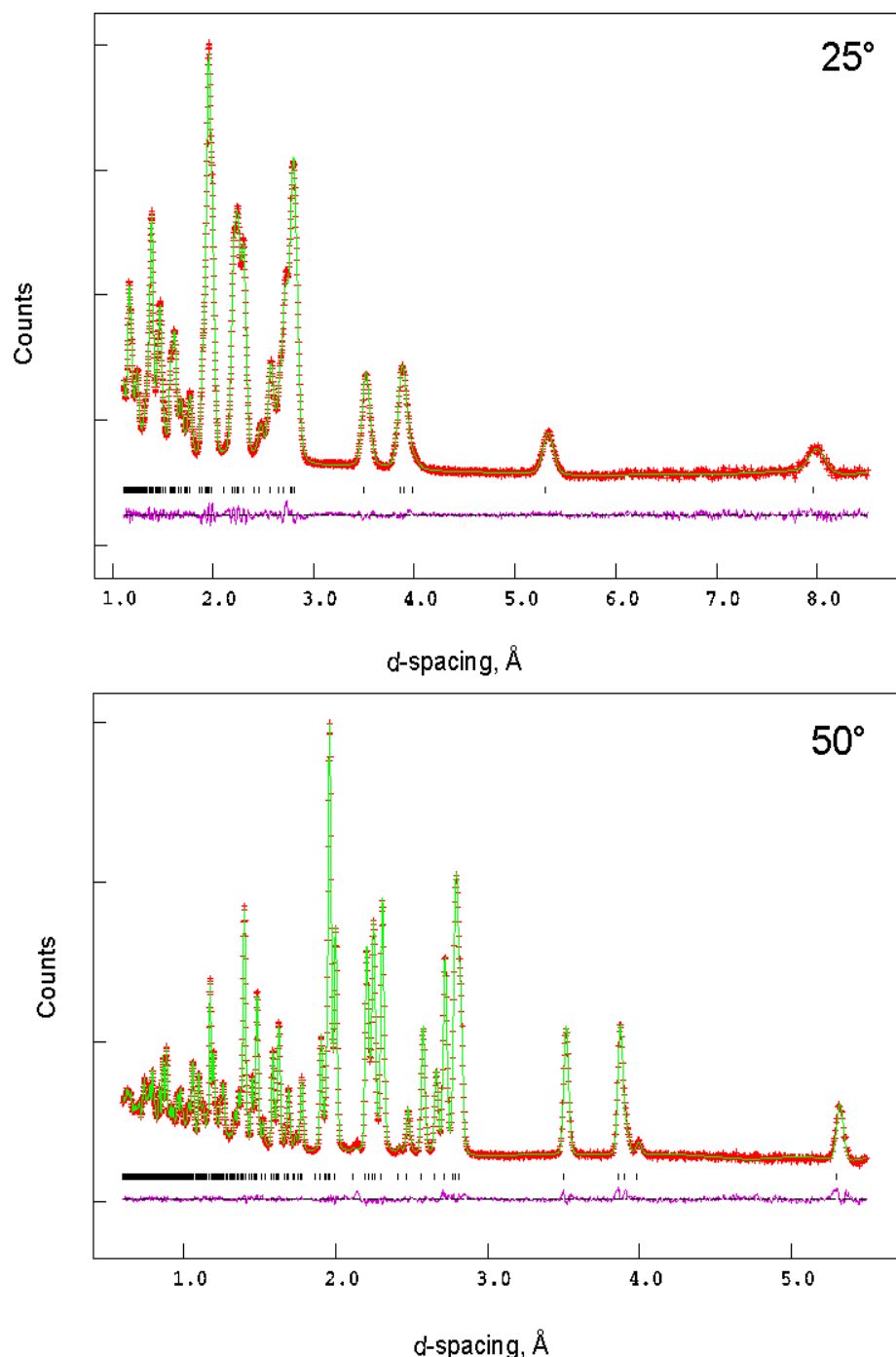


Figure S2a. Observed, calculated and difference plots from the refinement of $\text{La}_{0.6}\text{Sr}_{1.4}\text{CoGaO}_{5.02}$ against powder neutron diffraction data, 25° and 50° banks.

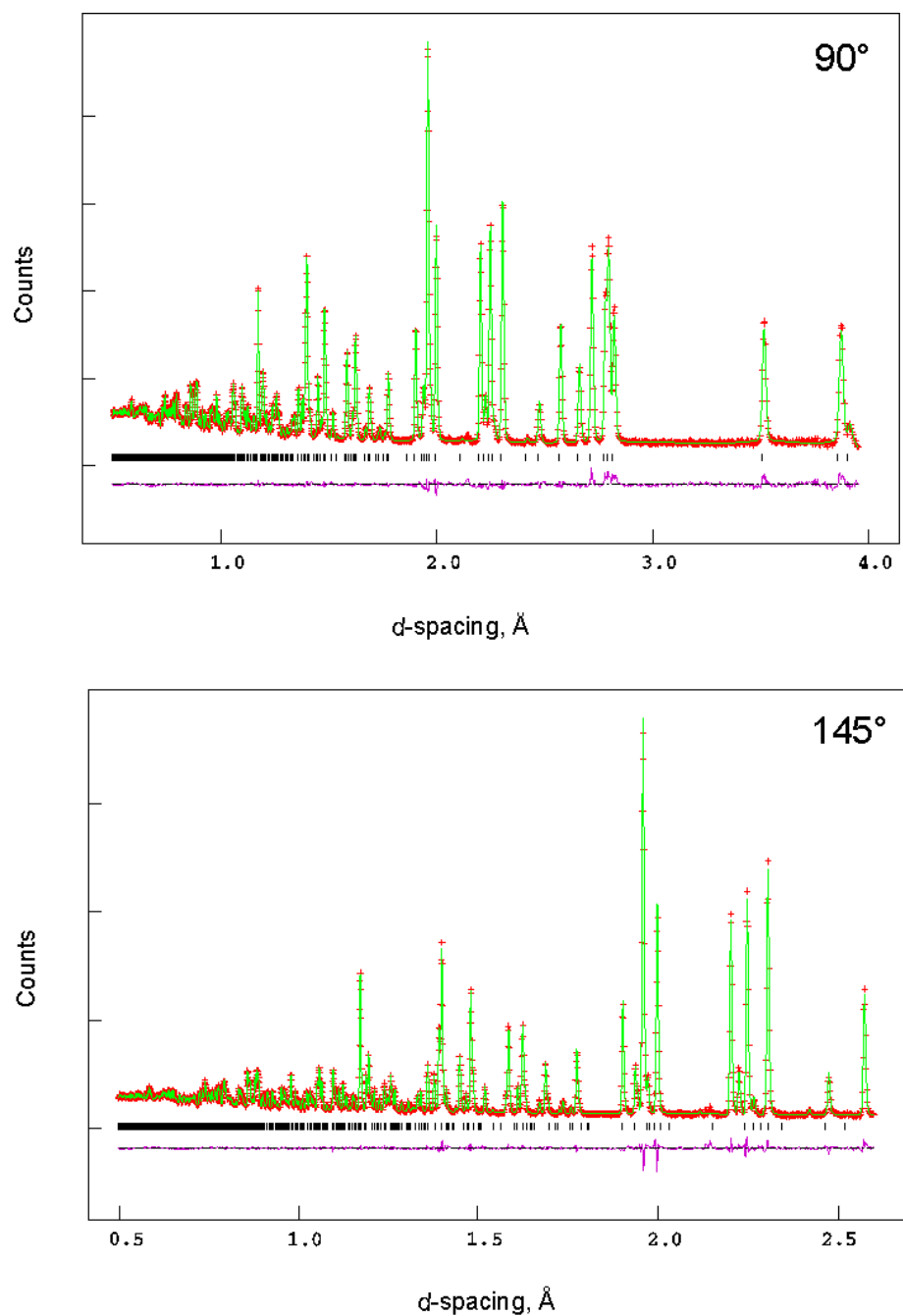


Figure S2b. Observed, calculated and difference plots from the refinement of $\text{La}_{0.6}\text{Sr}_{1.4}\text{CoGaO}_{5.02}$ against powder neutron diffraction data, 90° and 145° banks.

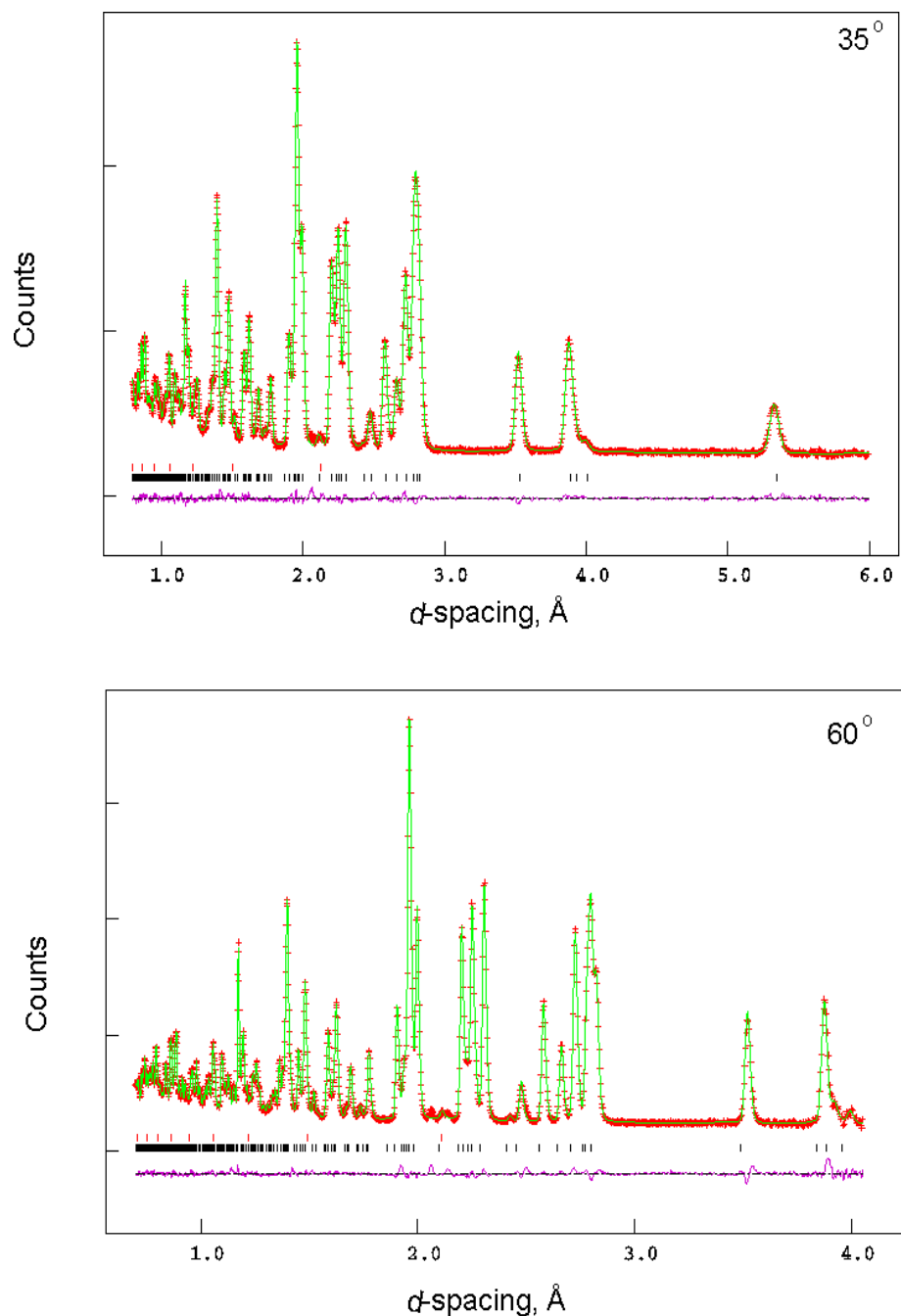


Figure S3a. Observed, calculated and difference plots from the refinement of $\text{La}_{0.7}\text{Sr}_{1.3}\text{CoGaO}_{5.05}$ against powder neutron diffraction data, 35° and 60° banks.

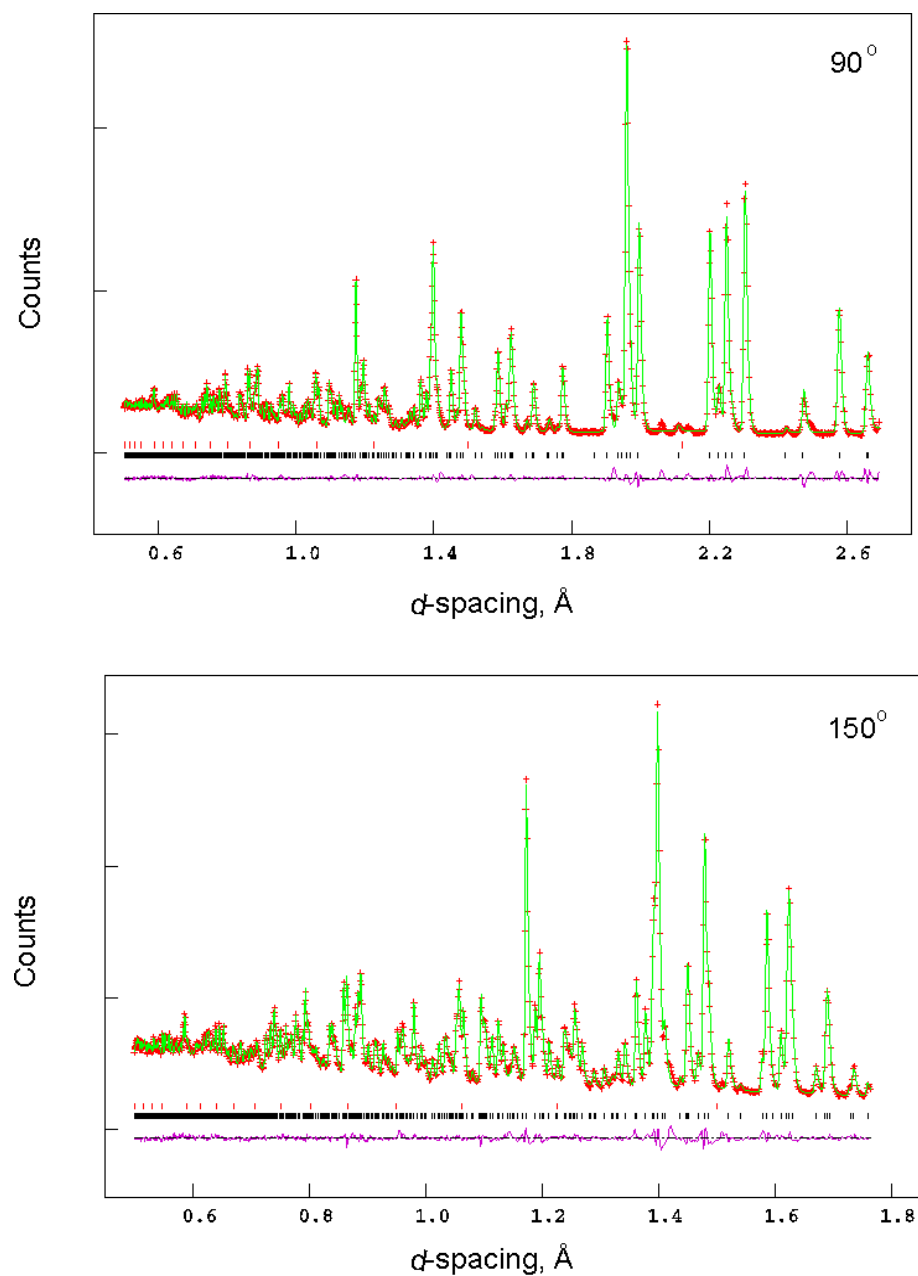


Figure S3b. Observed, calculated and difference plots from the refinement of $\text{La}_{0.7}\text{Sr}_{1.3}\text{CoGaO}_{5.05}$ against powder neutron diffraction data, 90° and 150° banks.

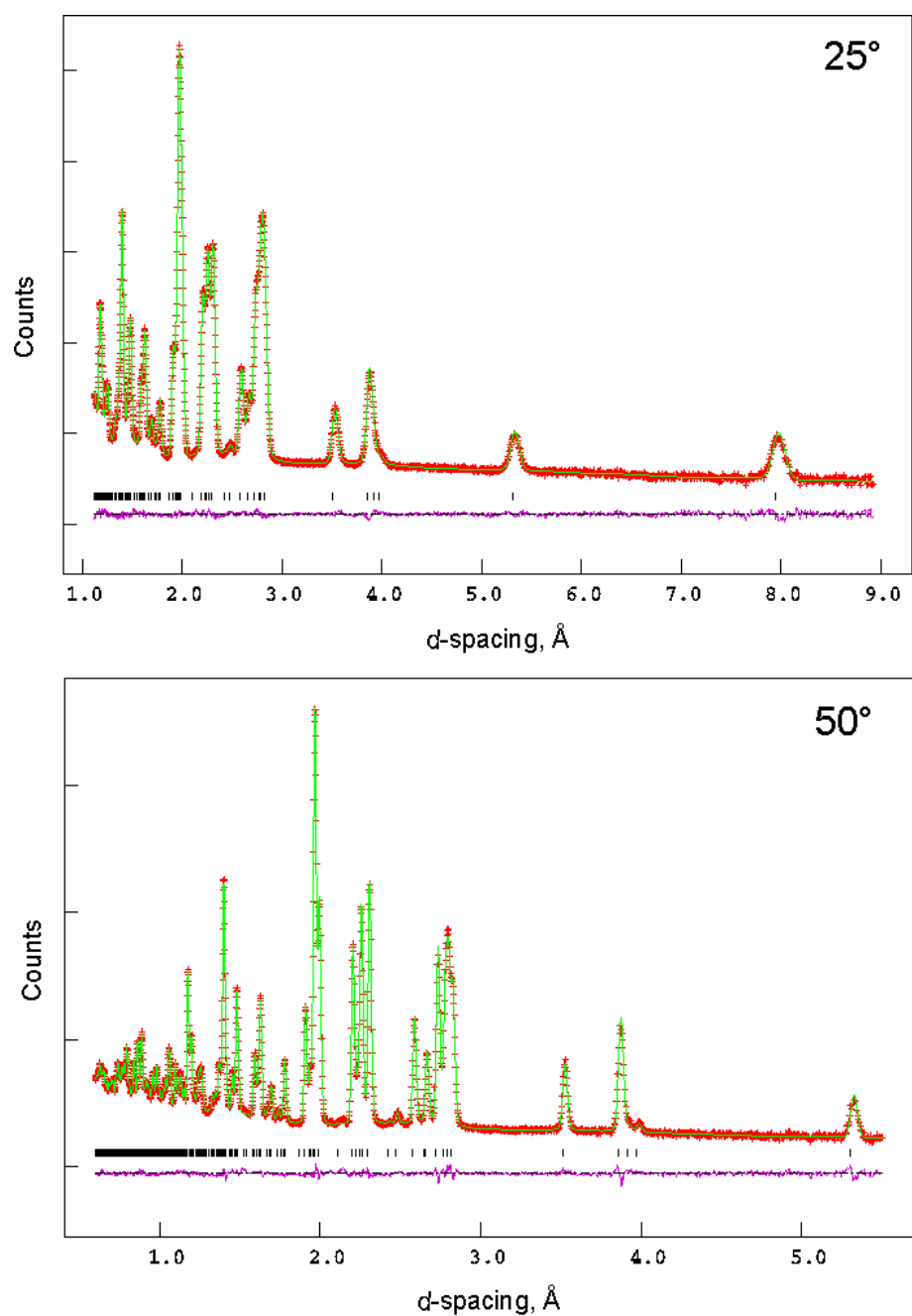


Figure S4a. Observed, calculated and difference plots from the refinement of $\text{La}_{0.8}\text{Sr}_{1.2}\text{CoGaO}_{5.09}$ against powder neutron diffraction data, 25° and 50° banks.

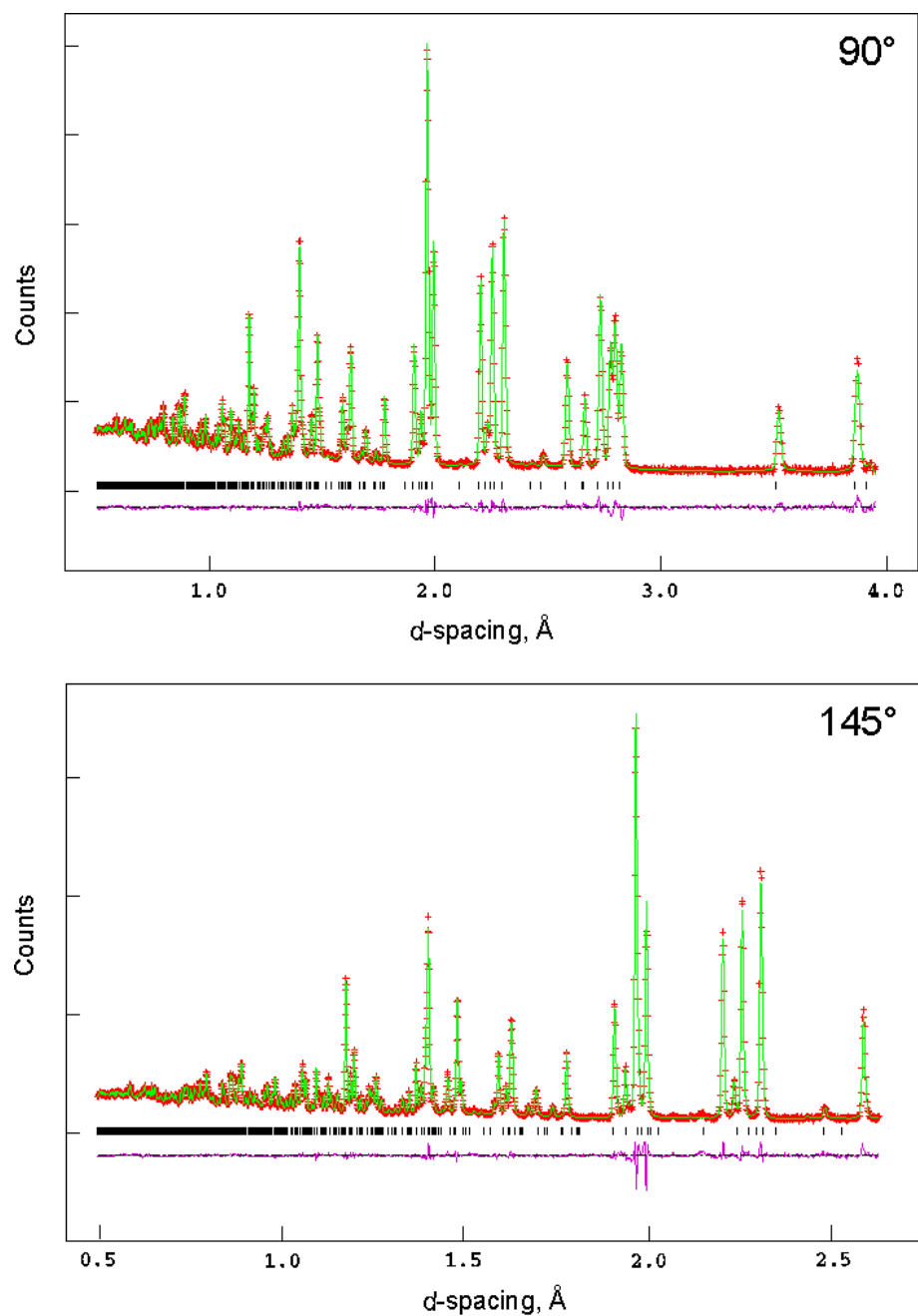


Figure S4b. Observed, calculated and difference plots from the refinement of $\text{La}_{0.8}\text{Sr}_{1.2}\text{CoGaO}_{5.09}$ against powder neutron diffraction data, 90° and 145° banks.

Composition		x = 0.5	x = 0.6	x = 0.7		x = 0.8
Co/Ga octahedral	Co/Ga(1)-O(1)×2	1.955(2)	1.952(2)	1.964(2)	Co/Ga(1)-O(1)×4	1.968(1)
	Co/Ga(1)-O(1)×2	1.964(2)	1.971(2)	1.964(2)	Co/Ga(1)-O(2)×2	2.329(2)
	Co/Ga(1)-O(2)×2	2.354(2)	2.357(2)	2.345(2)		
Co/Ga tetrahedral	Co/Ga(2)-O(2)×2	1.826(2)	1.829(2)	1.837(2)	Co/Ga(2)-O(2)×2	1.827(1)
	Co/Ga(2)-O(3)	1.890(1)	1.895(1)	1.898(2)	Co/Ga(2)-O(3)×2	1.911(1)
	Co/Ga(2)-O(3)	1.897(1)	1.903(1)	1.926(2)	Co/Ga(2)-O(4)	-
Tetrahedral twist (°)		52.87(2)	53.21(2)	53.61(2)		53.40(2)
Layer separation(Å)		7.9789(7)	7.9833(7)	7.9802(9)		7.9664(11)
Cation Ordered Fraction (%)		73.8	74.4	68.8		62.8

Table S6. Selected Bond Lengths (Å) and Angles (deg) from the refinement of $\text{La}_x\text{Sr}_{2-x}\text{CoGaO}_{5+\delta}$ phases

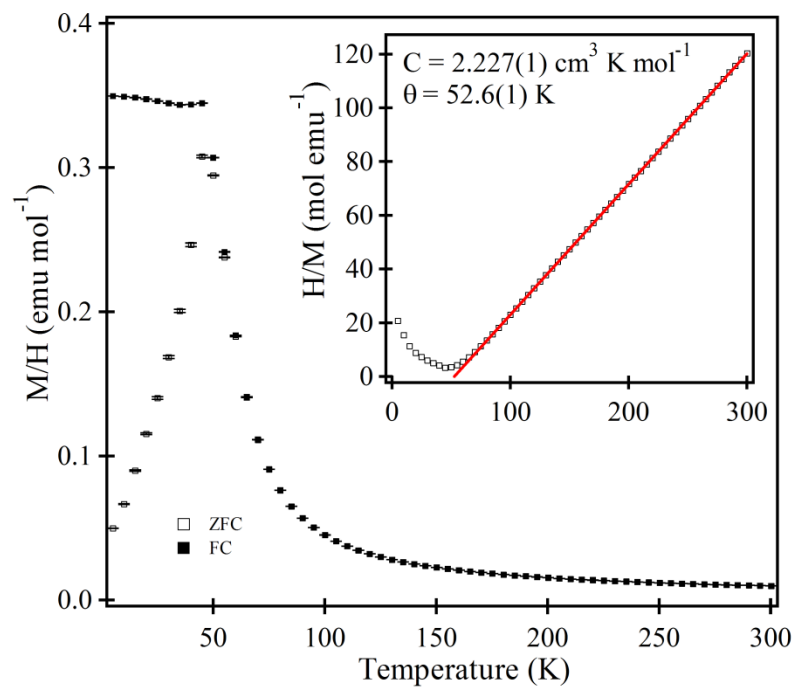


Figure S5. Zero field-cooled and field-cooled magnetisation data collected from $\text{La}_{0.5}\text{Sr}_{0.5}\text{CoGaO}_{5.01}$ as a function of temperature. Inset shows fit to the Curie-Weiss law.

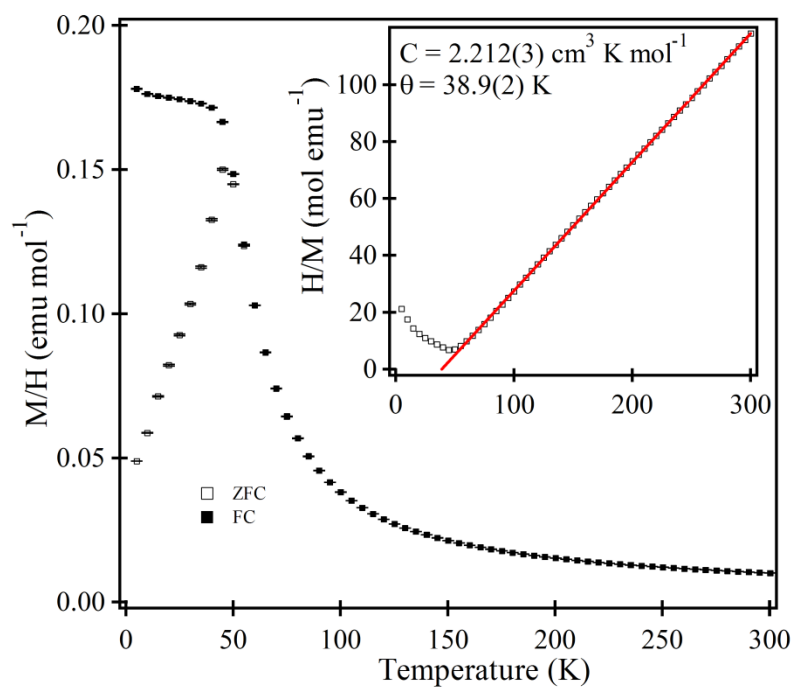


Figure S6. Zero field-cooled and field-cooled magnetisation data collected from $\text{La}_{0.6}\text{Sr}_{0.4}\text{CoGaO}_{5.02}$ as a function of temperature. Inset shows fit to the Curie-Weiss law.

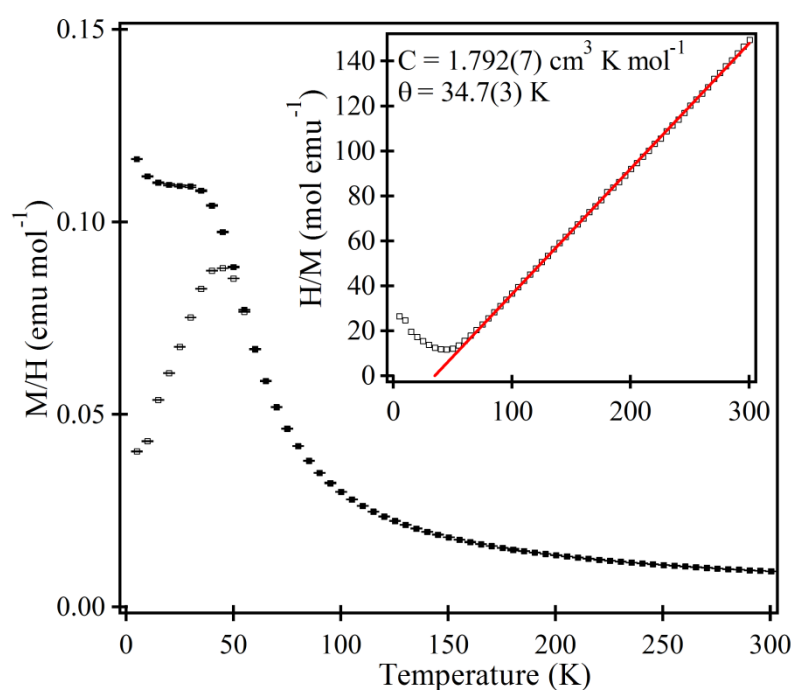


Figure S7. Zero field-cooled and field-cooled magnetisation data collected from $\text{La}_{0.7}\text{Sr}_{0.3}\text{CoGaO}_{5.05}$ as a function of temperature. Inset shows fit to the Curie-Weiss law.

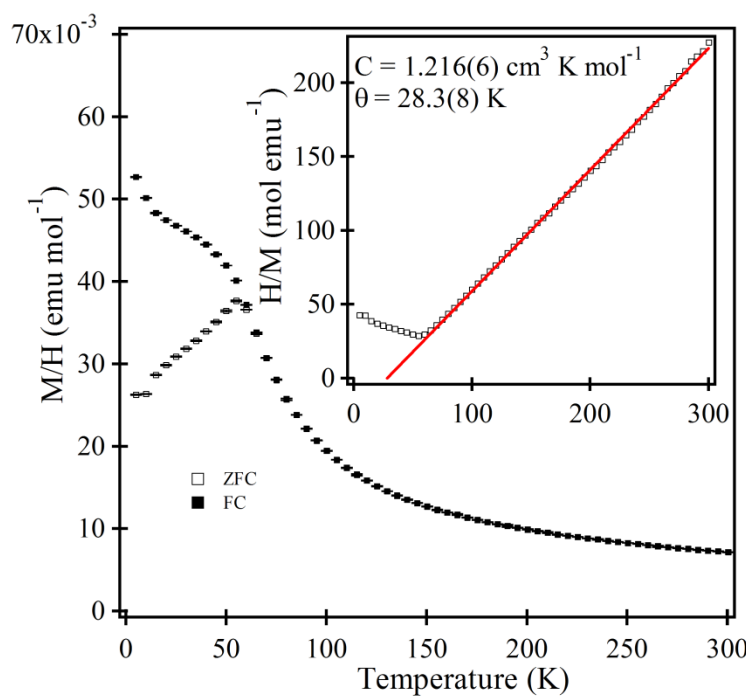


Figure S8. Zero field-cooled and field-cooled magnetisation data collected from $\text{La}_{0.8}\text{Sr}_{1.2}\text{CoGaO}_{5.09}$ as a function of temperature. Inset shows fit to the Curie-Weiss law.

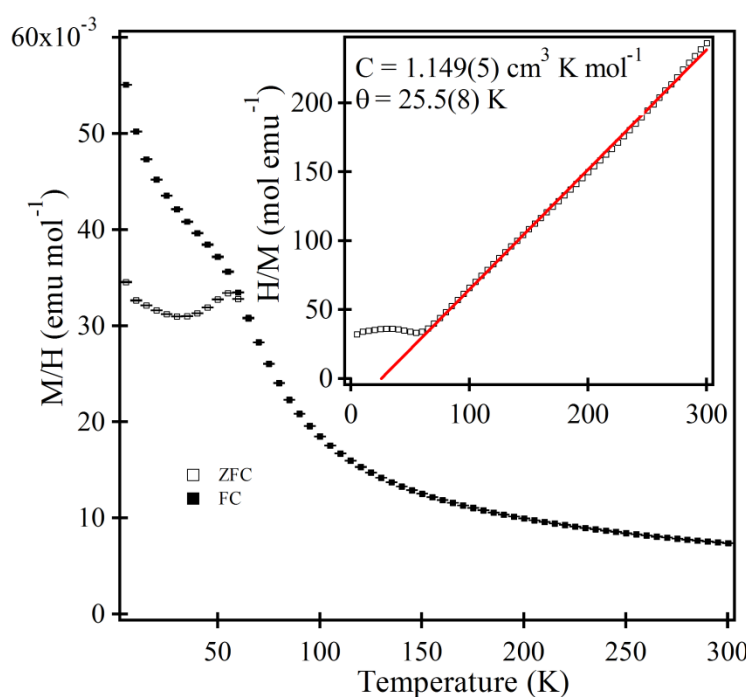


Figure S9. Zero field-cooled and field-cooled magnetisation data collected from $\text{LaSrCoGaO}_{5.18}$ as a function of temperature. Inset shows fit to the Curie-Weiss law.

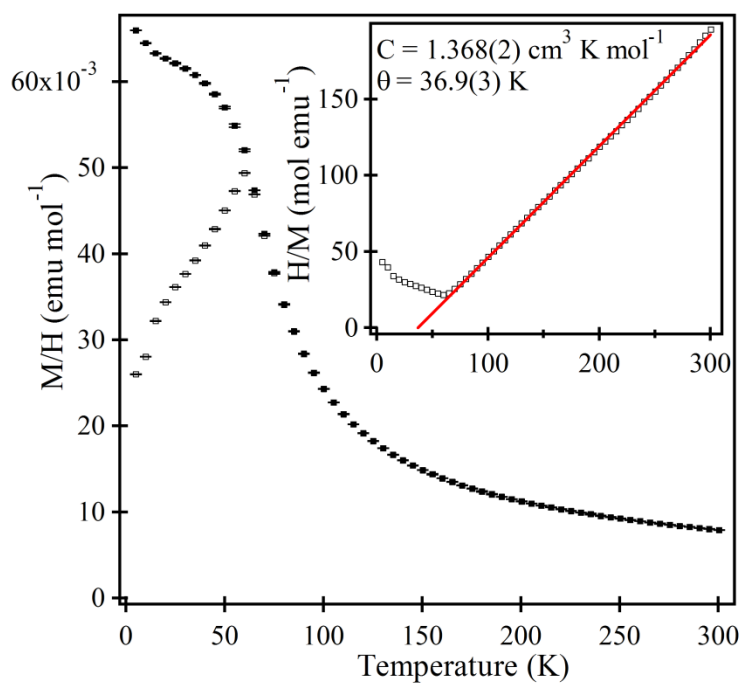


Figure S10. Zero field-cooled and field-cooled magnetisation data collected from $\text{La}_{0.7}\text{Sr}_{1.3}\text{CoGaO}_{5.02}$ as a function of temperature. Inset shows fit to the Curie-Weiss law.

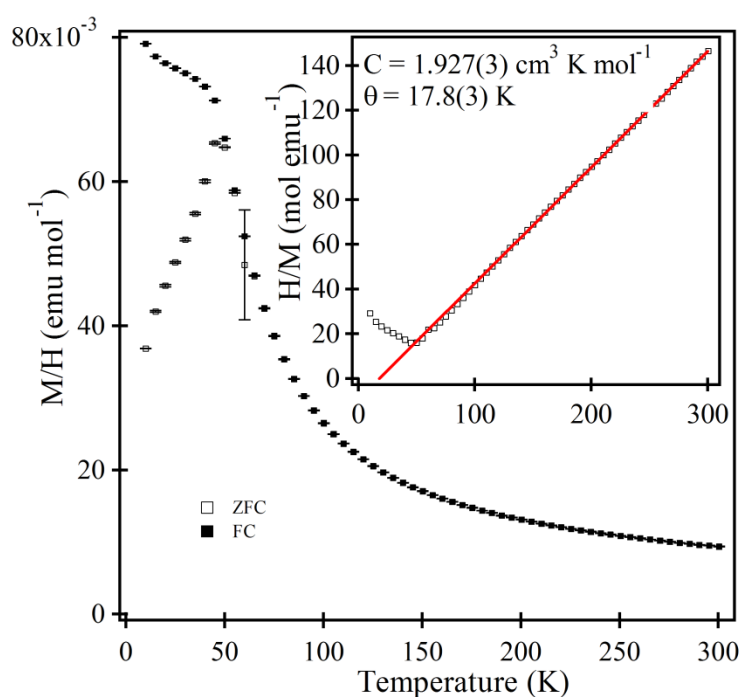


Figure S11. Zero field-cooled and field-cooled magnetisation data collected from $\text{La}_{0.8}\text{Sr}_{1.2}\text{CoGaO}_{5.16}$ as a function of temperature. Inset shows fit to the Curie-Weiss law.

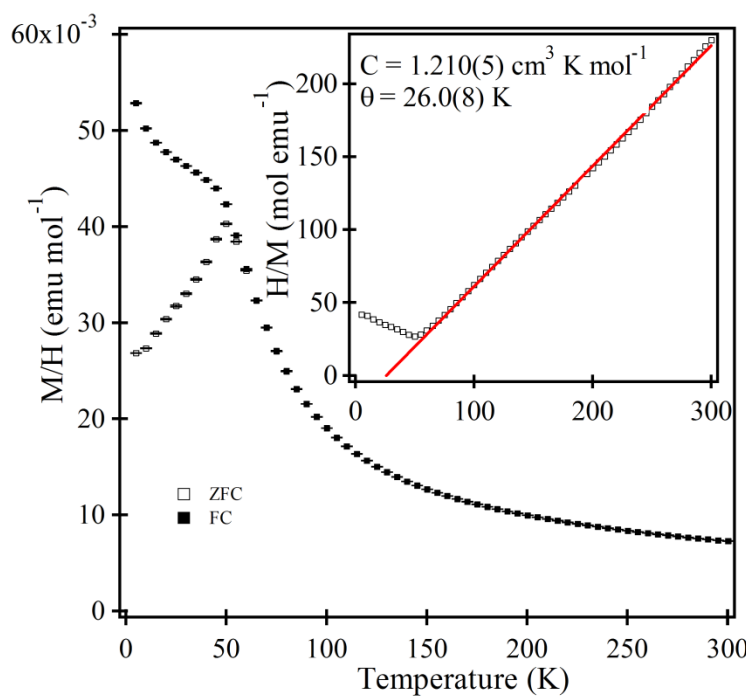


Figure S12. Zero field-cooled and field-cooled magnetisation data collected from $\text{La}_{0.9}\text{Sr}_{1.1}\text{CoGaO}_{5.13}$ as a function of temperature. Inset shows fit to the Curie-Weiss law.

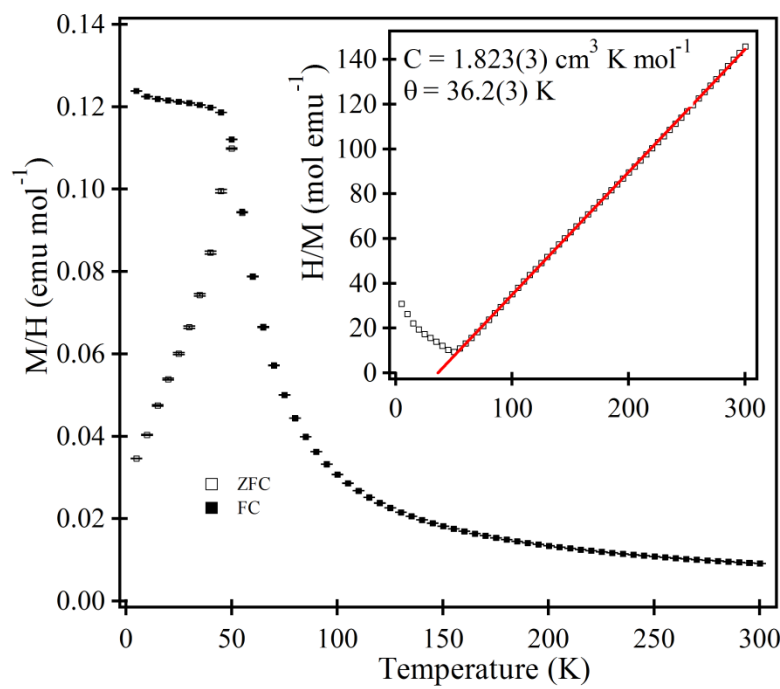


Figure S13. Zero field-cooled and field-cooled magnetisation data collected from $\text{La}_{0.7}\text{Sr}_{1.15}\text{Ca}_{0.15}\text{CoGaO}_{5.06}$ as a function of temperature. Inset shows fit to the Curie-Weiss law.

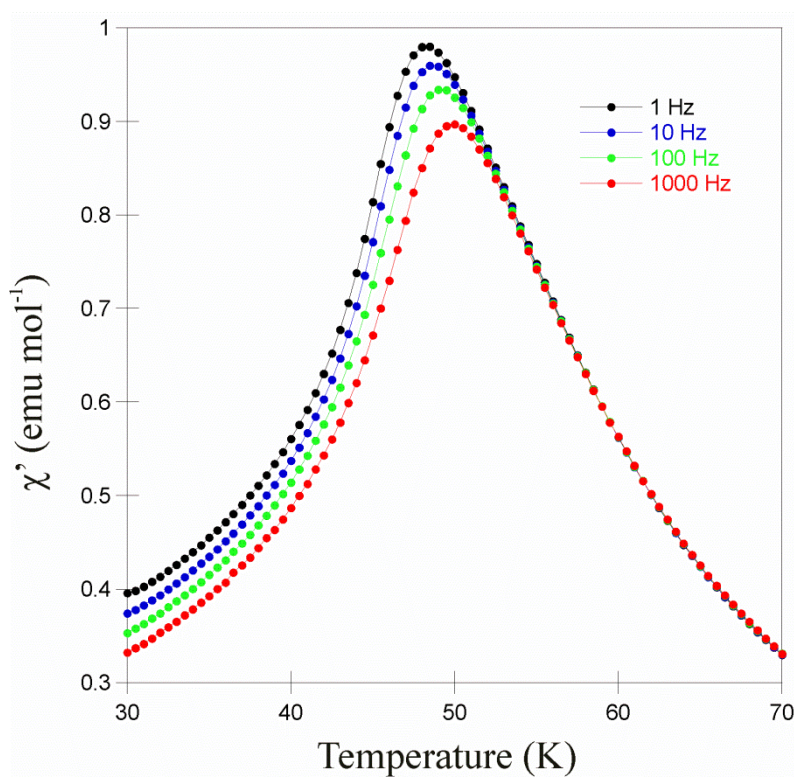


Figure S14. AC susceptibility data collected as a function of temperature from $\text{La}_{0.5}\text{Sr}_{1.5}\text{CoGaO}_{5.01}$ at 1, 10, 100 and 1000Hz.

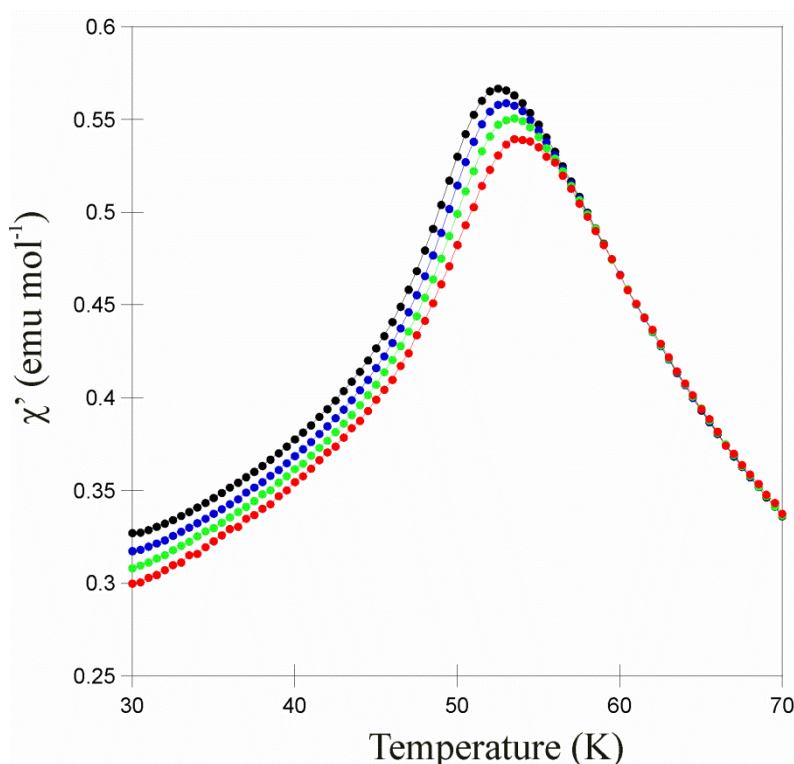


Figure S15. AC susceptibility data collected as a function of temperature from $\text{La}_{0.6}\text{Sr}_{1.4}\text{CoGaO}_{5.02}$ at 1, 10, 100 and 1000Hz.

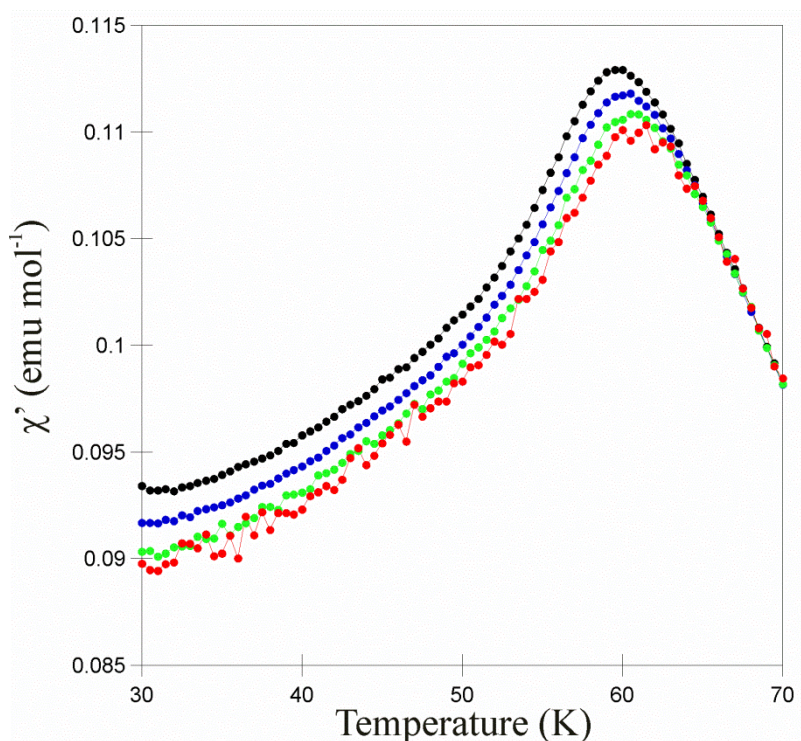


Figure S16. AC susceptibility data collected as a function of temperature from $\text{La}_{0.8}\text{Sr}_{1.2}\text{CoGaO}_{5.09}$ at 1, 10, 100 and 1000Hz.

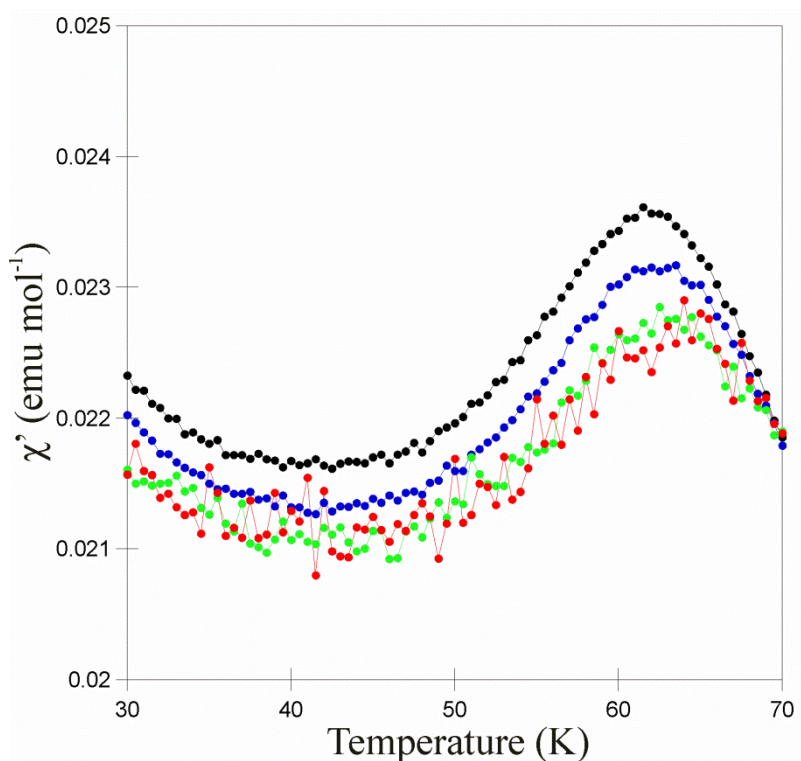


Figure S17. AC susceptibility data collected as a function of temperature from $\text{LaSrCoGaO}_{5.18}$ at 1, 10, 100 and 1000Hz.